ACKNOWLEDGMENT

This work was supported by EMW, Seoul, Korea.

REFERENCES

1. Wikipedia, the free encyclopedia. Available at: http://en.wikipedia.Org/wiki/LTE.
2. R.G. Vaughan and J.B. Anderson, Antenna diversity in mobile communications, IEEE Trans Veh Technol VT-36 (1987), 147–172.
3. T.-Y. Wu, S.-T. Fang, and K.-L. Wong, Printed diversity monopole antenna for WLAN operation, Electron Lett 38 (2002), 1625–1626.
4. Y. Ge, K.P. Esselle, and T.S. Bird, Compact diversity antenna for wireless devices, Electron Lett 41 (2005), 52–53.
5. K.-J. Kim and K.-H. Ahn, The high isolation dual-band inverted F antenna diversity system with the small N-section resonators on the ground plane, Microwave Opt Technol Lett 49 (2007), 731–734.
6. Computer Simulation Technology (CST) Microwave Studio. Suite 2009 [Online]. Available at: http://www.cst.com.
7. S. Blanch, J. Romeu, and I. Corbella, Exact representation of antenna system diversity performance from input parameter description, Electron Lett 39 (2003), 705–707.

WIDEBAND SURFACE-MOUNT CHIP ANTENNA FOR EIGHT-BAND LTE/WWAN SLIM MOBILE PHONE APPLICATION

Kin-Lu Wong and Cheng-Tse Lee
Department of Electrical Engineering, National Sun Yat-Sen University, Kaohsiung 80424, Taiwan; Corresponding author: wongkl@ema.ee.nsysu.edu.tw

Received 1 February 2010

ABSTRACT: *Surface-mount chip antenna with a thin thickness of 3 mm and a small volume of 3 × 4 × 50 mm^3 (0.6 cm^3) for eight-band long term evolution/wireless wide area network (LTE/WWAN) operation in the slim mobile phone is presented. The antenna is a simple two-strip shorted monopole, yet it can provide two wide operating bands of at least 698–960/1710–2690 MHz to cover the three LTE bands (LTE700/2300/2500) and five WWAN bands (GSM850/900/1800/1900/UMTS). The antenna is suitable to be mounted on the no-ground board space of the system circuit board of the mobile phone. Wideband operation is achieved by incorporating an on-board feeding structure formed by a short shorting strip and a chip capacitor–loaded feeding strip, both are of 8 mm in length and disposed on the no-ground board space, to the proposed chip antenna. Details of the antenna including the on-board feeding structure are presented.* © 2010 Wiley Periodicals, Inc.

Microwave Opt Technol Lett 52:2554–2560, 2010; View this article online at wileyonlinelibrary.com. DOI 10.1002/mop.25543

Key words: *mobile antennas; handset antennas; surface-mount chip antennas; LTE/WWAN antennas*

1. INTRODUCTION

Surface-mount chip antennas have been applied in the mobile phone as internal antennas for wireless wide area network (WWAN) operation [1–4]. Such surface-mount WWAN antennas are mainly mounted on the no-ground portion of the system circuit board of the mobile phone and can decrease the packaging cost of the internal antenna in the mobile phone. Recently, owing to the slim mobile phone becoming attractive for mobile users, the internal WWAN antennas to be embedded inside the mobile phone are required to have a thin profile [5–8]. In addition, wideband operation to cover the existing five WWAN operating bands (GSM850/900 and GSM1800/1900/UMTS, 824–960 and 1710–2170 MHz bands) and the new long term evolution (LTE) operation [9] in the LTE700 (698–787 MHz), LTE2300 (2300–2400 MHz), and LTE2500 (2500–2690 MHz) bands is required for some modern mobile phones. With both the WWAN and LTE operation, better and more seamless mobile broadband and multimedia services can be provided for the mobile users. Hence, eight-band LTE/WWAN operation in the 698–960/1710–2690 MHz bands will be demanded for the standard mobile phones in the very near future.

In this article, we present a promising wideband surface-mount chip antenna with a thin profile of 3 mm and a small footprint of 4 × 50 mm^2 for eight-band LTE/WWAN operation in the slim mobile phone. With 3-mm thickness, the proposed antenna can be easily embedded not only in the slim mobile phone but also in many modern mobile communication devices. For obtaining wideband operation and small volume, the proposed chip antenna uses a simple metal pattern of two-strip shorted monopole and a simple feeding structure formed by a short shorting strip and a chip capacitor–loaded feeding strip disposed on the no-ground portion of the system circuit board. Details of the chip antenna and the on-board feeding structure are introduced and the operating principle is discussed. Results for the antenna performances are also presented. The specific absorption rate (SAR) [10, 11] values for the proposed antenna with the presence of both the head and hand phantoms are also given.

2. PROPOSED ANTENNA

Figure 1(a) shows the geometry of the proposed wideband surface-mount chip antenna for eight-band LTE/WWAN slim mobile phone. The detailed dimensions of the antenna and the on-board feeding structure are given in Figure 1(b). The chip antenna has a total volume of 3 × 4 × 50 mm^3 or 0.6 cm^3 only and is supported by a foam base whose relative permittivity is close to unity in the study. A 0.8-mm-thick FR4 substrate of relative permittivity 4.4 and loss tangent 0.024 is used as the system circuit board of the mobile phone in the experiment. A ground plane of length 100 mm and width 50 mm is printed on the back surface of the circuit board as the system ground plane, and a no-ground board space of size 12 × 50 mm^2 on one edge of the circuit board is allocated for the chip antenna and the on-board feeding structure. To simulate the mobile phone housing, a plastic housing fabricated using a 1-mm-thick plastic slab of relative permittivity 3.0 and conductivity 0.01 S/m encloses the circuit board in the experiment.

The metal pattern of the chip antenna is unfolded as shown in Figure 1(b). The antenna is a simple two-strip monopole. The longer radiating strip has a length of 79 mm, while the shorter radiating strip has a length of 19 mm. Notice that in the longer radiating strip, there is a notched section for tuning the frequency ratio of the antenna's first two resonant modes such that the lowest mode is at about 850 MHz and the highest mode is at about 1900 MHz. Also, there is an embedded narrow slit of length (s) 17 mm and width (w) 0.5 mm to incorporate the simple shorting strip (section BD, length 8 mm) printed on-board to form an inductive shorting strip (section BD and DE) [12] for the antenna to achieve good dual-resonance excitation of the lowest mode contributed by the longer radiating strip. The chip capacitor (1.8 pF used in this study) loaded in the feeding strip also greatly helps to improve the impedance matching of the excited dual-resonance mode, which can have a wide operating band to cover the LTE700/GSM850/900 bands (698–960 MHz).

On the other hand, the shorter radiating strip contributes a resonant mode at about 2400 MHz, which incorporates the one

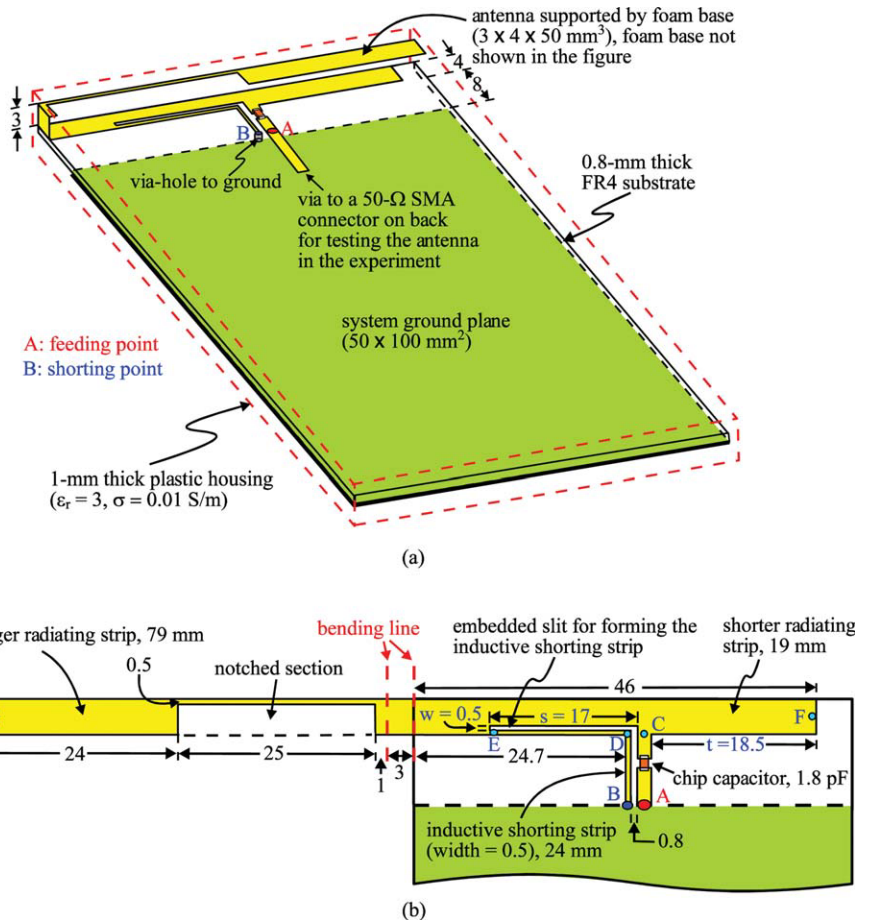

Figure 1 (a) Geometry of the proposed wideband surface-mount chip antenna for eight-band LTE/WWAN slim mobile phone. (b) Detailed dimensions of the antenna and the on-board feeding structure. [Color figure can be viewed in the online issue, which is available at wileyonlinelibrary.com]

generated by the longer radiating strip to form a wide operating band to cover the GSM1800/1900/UMTS/LTE2300/2500 bands (1710–2690 MHz). That is, the proposed chip antenna with the on-board feeding structure can provide two wide operating bands for eight-band LTE/WWAN operation (698–960/1710–2690 MHz). Note that the on-board feeding structure used in this study is much simpler than those applied in the coupled-fed planar inverted-F antennas or shorted monopoles that have been

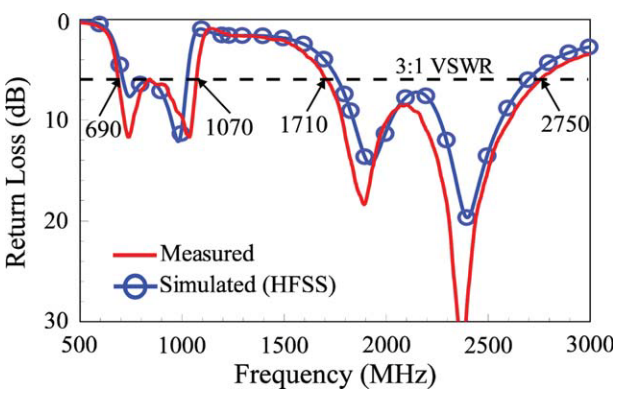

Figure 2 Measured and simulated return loss of the proposed antenna. [Color figure can be viewed in the online issue, which is available at wileyonlinelibrary.com]

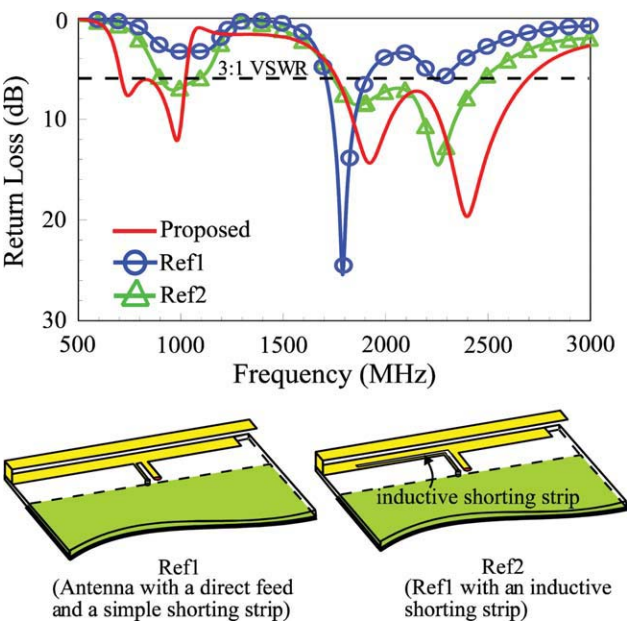

Figure 3 Simulated return loss for the proposed antenna, the corresponding antenna with a direct feed and a simple shorting strip (Ref1), and the corresponding antenna with a direct feed and an inductive shorting strip (Ref2). [Color figure can be viewed in the online issue, which is available at wileyonlinelibrary.com]

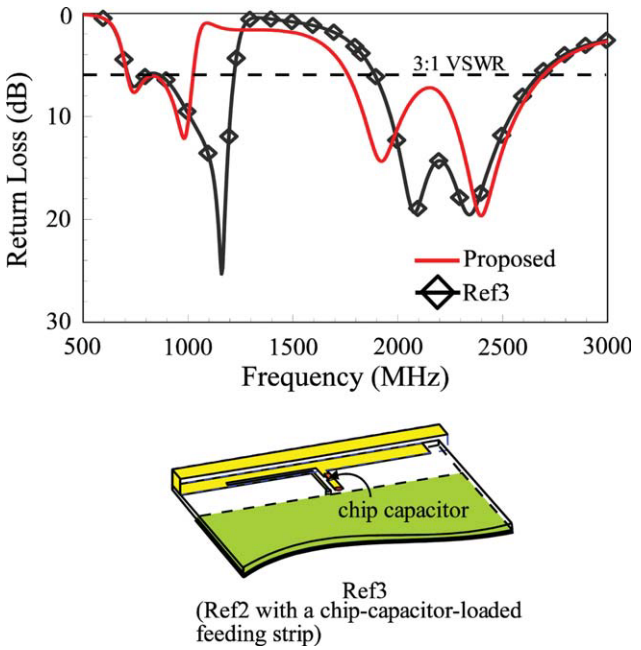

Figure 4 Simulated return loss of the corresponding antenna with an inductive shorting strip and a chip capacitor–loaded feeding strip (Ref3). [Color figure can be viewed in the online issue, which is available at wileyonlinelibrary.com]

reported for WWAN mobile phone applications [13–18]. In addition, widened bandwidths are further achieved for the proposed chip antenna for eight-band LTE/WWAN operation.

3. RESULTS AND DISCUSSION

The proposed chip antenna was fabricated and tested. Results of the measured and simulated return loss are shown in Figure 2. The simulated results are obtained using Ansoft simulation software HFSS version 12 [19], and good agreement between the measurement and simulation is seen. The wide lower and upper bands for the proposed antenna are obtained. The lower band shows a wide bandwidth of 380 MHz (690–1070 MHz), while the upper band has an even wide bandwidth of 1040 MHz (1710–2750 MHz). The two wide operating bands can cover the desired eight-band LTE/WWAN operation in the 698–960/1710–2690 MHz bands. Notice that the bandwidth definition of 3:1 VSWR (6-dB return loss) is widely used as the design specification for the internal WWAN mobile phone antennas.

To analyze the operating principle of the proposed antenna and the on-board feeding structure, the comparison of the simulated return loss for the proposed antenna, the corresponding antenna with a direct feed and a simple shorting strip (Ref1), the corresponding antenna with a direct feed and an inductive shorting strip (Ref2), and the corresponding antenna with an inductive shorting strip and a chip capacitor–loaded feeding strip (Ref3) is presented in Figures 3 and 4. Notice that Ref2 is Ref1 with an inductive shorting strip, and Ref3 is Ref2 with a chip capacitor–loaded feeding strip. The configurations of Ref1, Ref2, and Ref3 are also shown in the inset of Figures 3 and 4. From the results, it can be seen that Ref1 shows three resonant modes excited; however, the lowest one is at about 1000 MHz and with poor impedance matching, while the other two modes cannot be formed into a wide upper band for the antenna. With the inductive shorting strip formed for Ref2, the impedance matching for the lowest mode (the fundamental mode contributed by the longer radiating strip) at about 1000 MHz is improved, although it still cannot cover the desired lower band of 698–960 MHz. The other two modes are formed into a wide upper band for the antenna, and the obtained upper-band bandwidth is close to the desired bandwidth of 1710–2690 MHz. This impedance matching improvement for the three excited resonant modes can be explained more clearly from the simulated input impedance of Ref1 and Ref2 as shown in Figure 5(a), in which the lower impedance level that causes poor impedance matching for the three excited resonant modes is increased for Ref2. This is mainly because the embedded slit in the longer radiating strip for forming the inductive shorting strip also changes the shorting position of the chip antenna from point D to point E. Hence, the real and imaginary parts of the input

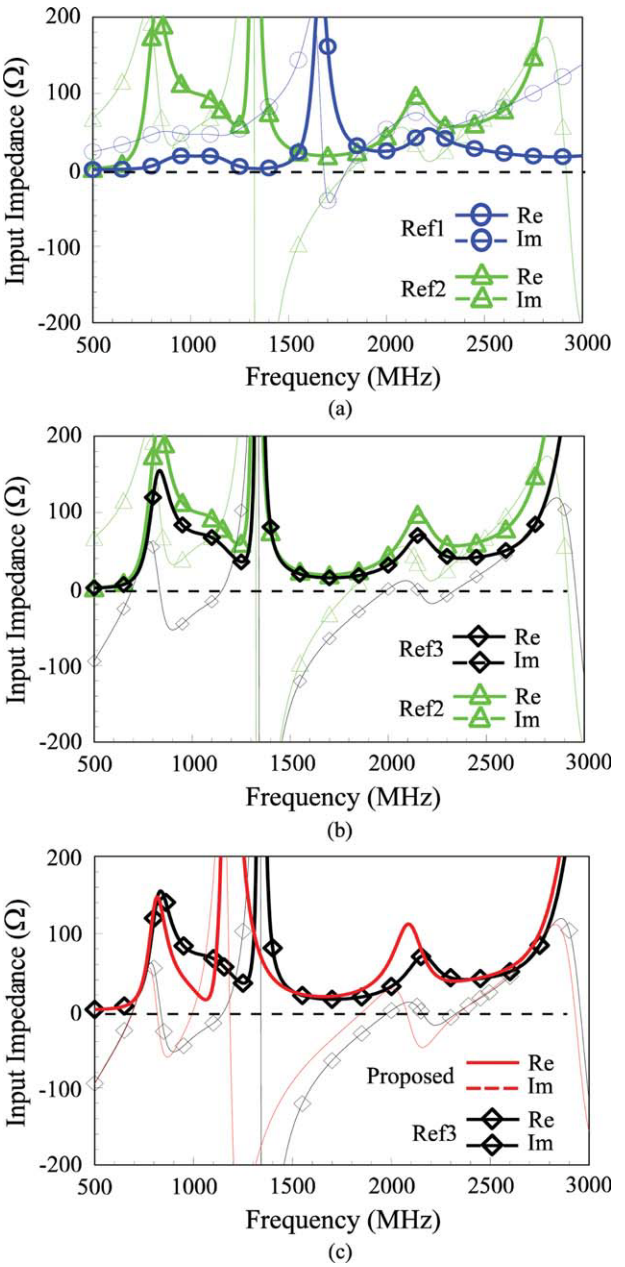

Figure 5 Comparison of the simulated input impedance for the antennas studied in Figures 3 and 4. (a) Ref1 and Ref2. (b) Ref2 and Ref3. (c) Ref3 and proposed antenna. [Color figure can be viewed in the online issue, which is available at wileyonlinelibrary.com]

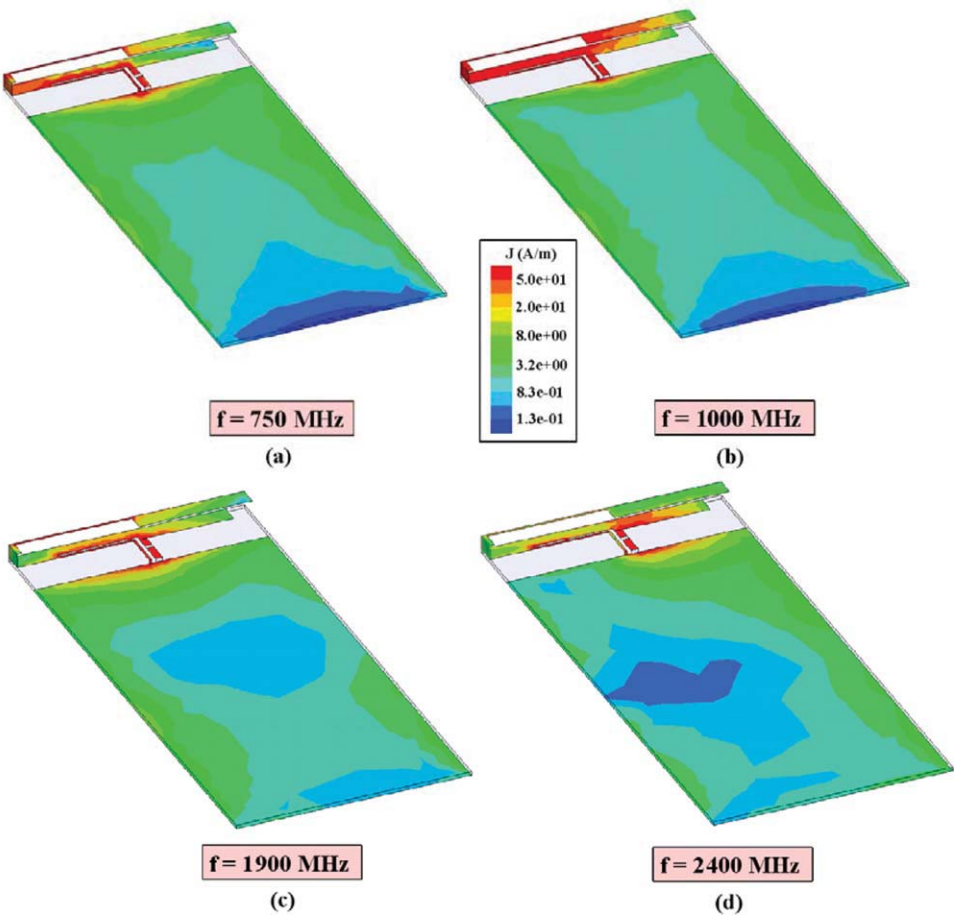

Figure 6 Simulated surface current distributions for the proposed antenna at (a) 750 MHz, (b) 1000 MHz, (c) 1900 MHz, and (d) 2400 MHz. [Color figure can be viewed in the online issue, which is available at wileyonlinelibrary.com]

impedance of the three excited resonant modes can both be increased to improve their impedance matching.

In Figure 4, it is seen that good dual-resonance excitation of the lowest mode is achieved for Ref3. This is mainly because the embedded chip capacitor of 1.8 pF in the feeding strip compensates for the large inductive reactance seen for Ref2 [see the results in Fig. 5(b)]. However, some effects on the other two modes are also observed, which slightly decrease the obtained bandwidth of the antenna's upper band. By further introducing a simple notched section in the longer radiating strip (see Fig. 1), as seen in Figure 5(c), the resonance (zero reactance) of the second mode (the higher-order mode contributed by the longer radiating strip) is shifted to lower frequencies, while that of the third mode contributed by the shorter radiating strip is generally not affected. This leads to a widened bandwidth for the antenna's upper band to cover the desired 1710–2690 MHz band.

The simulated surface current distributions for the proposed antenna are also shown in Figure 6. At 750 and 1000 MHz, similar surface current distributions on the longer radiating strip are seen, which confirm that the two resonances in the antenna's lower band are both contributed by the longer radiating strip. At 1900 MHz, there is current null in the surface currents on the longer radiating strip; this confirms that the second mode is the higher-order mode of the longer radiating strip. At 2400 MHz, strong surface currents on the shorter radiating strip are seen, which indicate that the third mode is mainly contributed by the shorter radiating strip.

Effects of the length s and width w of the embedded slit in the longer radiating strip are studied in Figure 7. Results of the simulated return loss for the length s varied from 0 to 21 mm are shown in Figure 7(a), while those for the width w varied from 0.2 to 0.8 mm are shown in Figure 7(b). It is seen that the length s greatly affects the impedance matching for frequencies over the three excited resonant modes. On the other hand, the width w mainly affects the impedance matching on the first mode (the lowest mode), and results indicate that the width w should not be too small such that the coupling between the embedded slit and the longer radiating strip can be ignored. From the parametric study, the preferred length s and width w are selected to be 17 and 0.5 mm, respectively, in the study.

Effects of the length t of the shorter radiating strip are shown in Figure 8. Results for the length t varied from 14.5 to 22.5 mm are presented. It is clearly seen that the third mode is strongly controlled by the length t; the third mode is shifted to higher frequencies with a decrease in the length t. This also confirms that the third mode is contributed by the shorter radiating strip.

The radiation characteristics of the fabricated antenna are also studied. Figure 9 plots the measured three-dimensional total-power radiation patterns. For lower frequencies (750 and 925 MHz), half-wavelength dipole-like radiation patterns are seen. For higher frequencies (1795, 2045, and 2500 MHz), there is a dip seen in the azimuthal plane (x-y plane), and the radiation patterns are close to those of the dipole antenna at its higher-order modes. This also

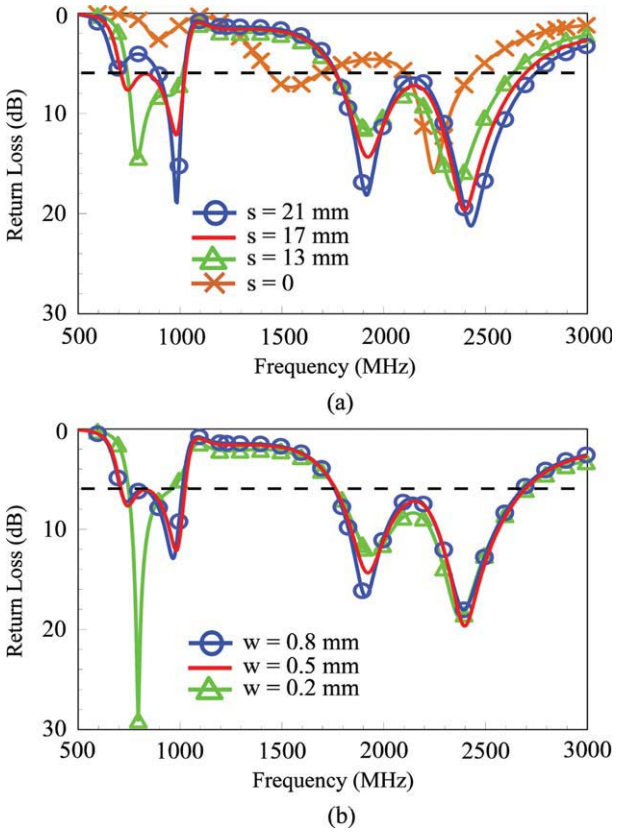

Figure 7 Simulated return loss as a function of (a) the length s and (b) the width w of the embedded slit for forming the inductive shorting strip. Other dimensions are the same as given in Figure 1. [Color figure can be viewed in the online issue, which is available at wileyonlinelibrary.com]

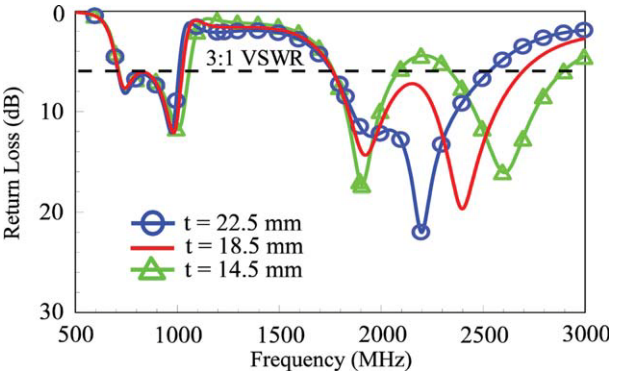

Figure 8 Simulated return loss as a function of the length t of the shorter radiating strip. Other dimensions are the same as given in Figure 1. [Color figure can be viewed in the online issue, which is available at wileyonlinelibrary.com]

suggests that the ground plane greatly controls the radiation patterns of the antenna, similar to those observed for the traditional internal WWAN mobile phone antennas [20]. Figure 10 shows the measured radiation efficiency and antenna gain of the fabricated antenna. The radiation efficiency for the lower and upper band is about 50–83% and 60–96%, respectively, while the antenna gain is about −1.0–1.5 dBi and 2.0–4.8 dBi, respectively.

The SAR results of the antenna are studied using the SAR simulation model provided by SEMCAD [21] as shown in Figure 11. The simulated SAR values for 1-g head and 1-g head/hand tissues are also given in the figure. The return loss at the testing frequency is also given. Note that the antenna is positioned at the bottom of the mobile phone, which has been shown to be a promising arrangement for practical applications of such antennas with no background plane to achieve decreased SAR values [11, 22–24]. The grip of the hand phantom on the tested mobile phone is shown in Figure 11, and the distance between the palm center and the housing is selected to be 30 mm; the distance is reasonable for testing the SAR values [11]. The input power for testing the SAR is 24 dBm for the GSM850/900 bands (859 and 925 MHz) and 21 dBm for the GSM1800/1900 bands (1795 and 1920 MHz), UMTS band (2045 MHz), and LTE bands (740, 2350, and

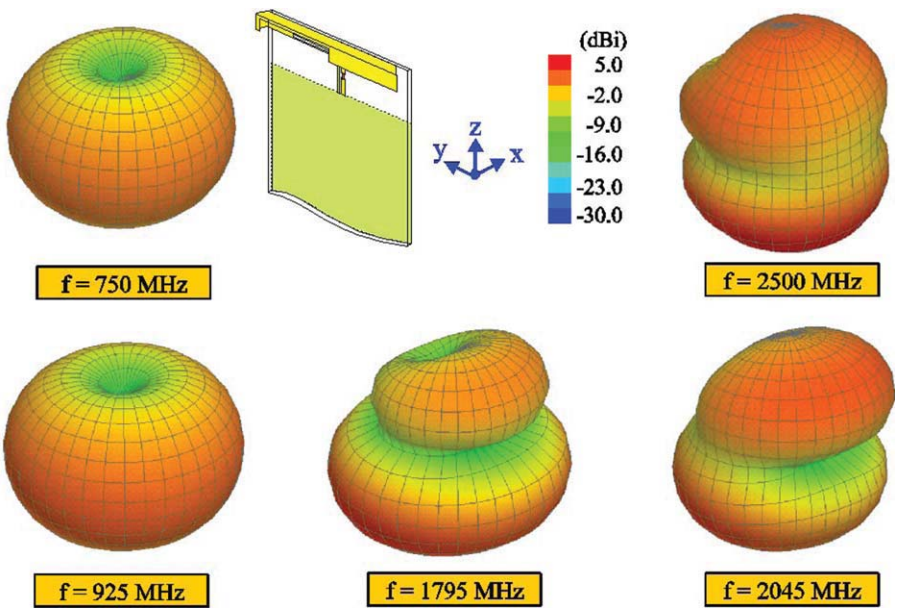

Figure 9 Measured three-dimensional (3D) radiation patterns for the proposed antenna. [Color figure can be viewed in the online issue, which is available at wileyonlinelibrary.com]

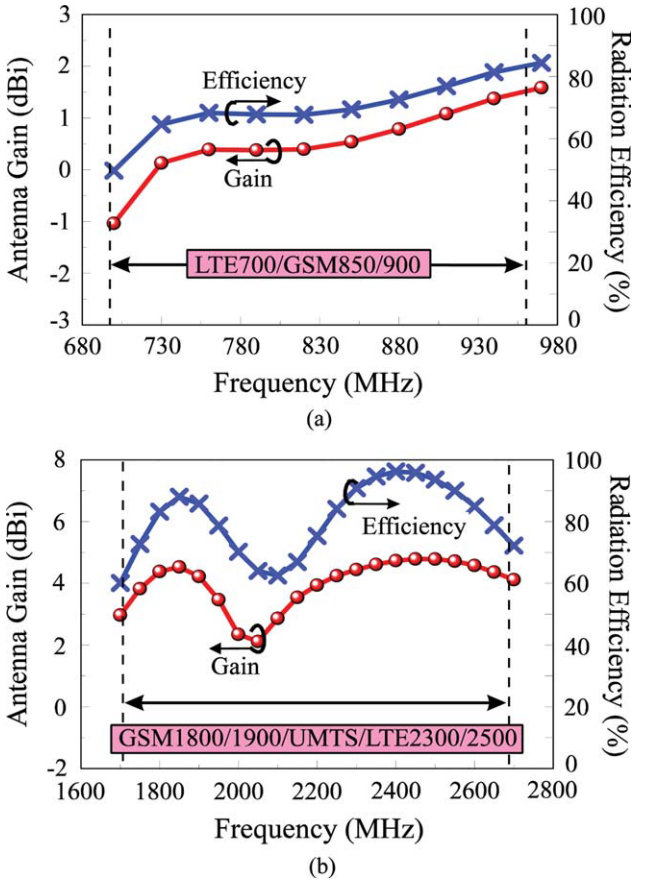

Figure 10 Measured radiation efficiency and antenna gain of the proposed antenna. [Color figure can be viewed in the online issue, which is available at wileyonlinelibrary.com]

2595 MHz). For the case of head only, the obtained SAR values over the operating bands all meet the limit of 1.6 W/kg [10]. When the hand phantom is present, small variations in the SAR values are seen for frequencies (740, 859, and 925 MHz) in the lower band. Small variations are also seen at 1795 and 1920 MHz. When the testing frequency increases further, the SAR values start to rapidly increase, especially at 2350 and 2595 MHz. The SAR values with the head and hand are three times higher than those with the head only. This is probably because the operating wavelengths of the higher frequencies become comparable to the dimensions of the fingers of the hand phantom, thus resulting in larger power absorption of the antenna. When the user's hand is required to be considered in the SAR testing for the mobile phone in the near future, the decrease in the SAR values for 1-g head/hand tissue at higher frequencies will be needed for the proposed antenna in practical applications.

4. CONCLUSIONS

A thin surface-mount chip antenna occupying a small volume of 0.6 cm^3 for eight-band LTE/WWAN operation in the slim mobile phone is presented. The chip antenna incorporates an on-board feeding structure formed by a shorting strip and a chip capacitor–loaded feeding strip to generate two wide operating bands to cover, respectively, the LTE700/GSM850/900 operation and the GSM1800/1900/UMTS/LTE2300/2500 operation. The operating principles of the antenna and the on-board feeding structure have been discussed, and good radiation characteristics for frequencies over the eight operating bands have been observed. The simulated SAR values for the proposed antenna positioned at the bottom of the system circuit board of the mobile phone and with the presence of the head and hand phantoms have also been analyzed.

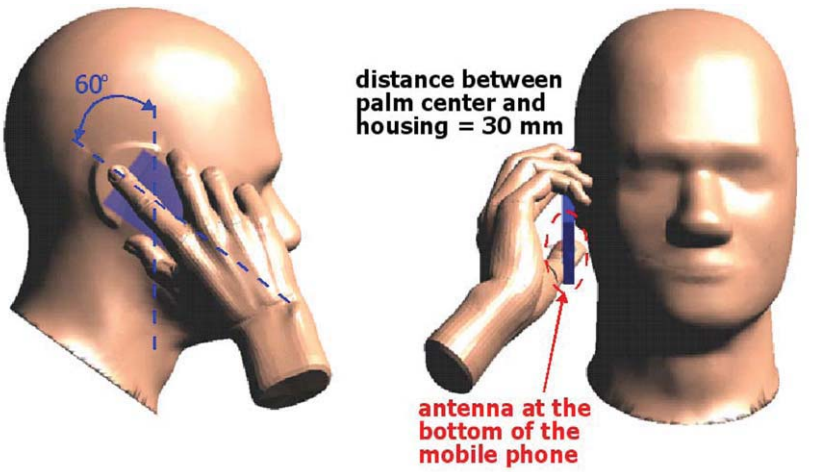

Frequency (MHz)		740	859	925	1795	1920	2045	2350	2595
1-g SAR (W/kg)	head only	0.65	1.35	1.54	1.01	0.98	0.81	0.71	0.65
	head and hand	0.56	1.55	1.58	1.15	0.87	0.98	2.68	2.06
Return loss (dB)	head only	12.8	8.4	10.8	10.7	27.1	10.4	13.2	7.2
	head and hand	11.1	9.6	11.0	16.3	16.7	9.0	13.6	7.2

Figure 11 SAR simulation model and the simulated SAR values for the proposed antenna. The return loss given in the table is the impedance matching level at the testing frequency. [Color figure can be viewed in the online issue, which is available at wileyonlinelibrary.com]

REFERENCES

1. C.L. Tang and S.C. Lai, Multi-function IC antenna design and fabrication, In: Proc Asia-Pacific Microwave Conf, Singapore, 2009, Session TU4A, Paper no. 1741.
2. Y.W. Chi and K.L. Wong, Compact multiband folded loop chip antenna for small-size mobile phone, IEEE Trans Antennas Propag 56 (2008), 3797–3803.
3. M.R. Hsu and K.L. Wong, WWAN ceramic chip antenna for mobile phone application, Microwave Opt Technol Lett 51 (2009), 103–110.
4. M.R. Hsu and K.L. Wong, Seven-band folded-loop chip antenna for WWAN/WLAN/WiMAX operation in the mobile phone, Microwave Opt Technol Lett 51 (2009), 543–549.
5. H. Rhyu, J. Byun, F.J. Harakiewicz, M.J. Park, K. Jung, D. Kim, N. Kim, T. Kim, and B. Lee, Multi-band hybrid antenna for ultra-thin mobile phone applications, Electron Lett 45 (2009), 773–334.
6. R.A. Bhatti, Y.T. Im, J.H. Choi, T.D. Manh, and S.O. Park, Ultra-thin planar inverted-F antenna for multistandard handsets, Microwave Opt Technol Lett 50 (2008), 2894–2897.
7. K.L. Wong, Y.C. Lin, and T.C. Tseng, Thin internal GSM/DCS patch antenna for a portable mobile terminal, IEEE Trans Antennas Propag 54 (2006), 238–242.
8. K.L. Wong, Y.C. Lin, and B. Chen, Internal patch antenna with a thin air-layer substrate for GSM/DCS operation in a PDA phone, IEEE Trans Antennas Propag 55 (2007), 1165–1172.
9. S. Sesia, I. Toufik, and M. Baker (Eds.), LTE, The UMTS long term evolution: From theory to practice, Wiley, New York, 2009.
10. American National Standards Institute (ANSI), Safety levels with respect to human exposure to radio-frequency electromagnetic field, 3 kHz to 300 GHz, ANSI/IEEE Standard C95.1, Apr. 1999.
11. C.H. Li, E. Ofli, N. Chavannes, and N. Kuster, Effects of hand phantom on mobile phone antenna performance, IEEE Trans Antennas Propag 57 (2009), 2763–2770.
12. C.H. Chang and K.L. Wong, Small-size printed monopole with a printed distributed inductor for penta-band WWAN mobile phone application, Microwave Opt Technol Lett 51 (2009), 2903–2908.
13. K.L. Wong and C.H. Huang, Bandwidth-enhanced internal PIFA with a coupling feed for quad-band operation in the mobile phone, Microwave Opt Technol Lett 50 (2008), 683–687.
14. K.L. Wong and C.H. Huang, Printed PIFA with a coplanar coupling feed for penta-band operation in the mobile phone, Microwave Opt Technol Lett 50 (2008), 3181–3186.
15. C.H. Chang and K.L. Wong, Internal coupled-fed shorted monopole antenna for GSM850/900/1800/1900/UMTS operation in the laptop computer, IEEE Trans Antennas Propag 56 (2008), 3600–3604.
16. K.L. Wong and S.J. Liao, Uniplanar coupled-fed printed PIFA for WWAN operation in the laptop computer, Microwave Opt Technol Lett 51 (2009), 549–554.
17. K.L. Wong and C.H. Huang, Compact multiband PIFA with a coupling feed for internal mobile phone antenna, Microwave Opt Technol Lett 50 (2008), 2487–2491.
18. C.T. Lee and K.L. Wong, Uniplanar coupled-fed printed PIFA for WWAN/WLAN operation in the mobile phone, Microwave Opt Technol Lett 51 (2009), 1250–1257.
19. Ansoft Corporation HFSS, Available at: http://www.ansoft.com/products/hf/hfss/.
20. K.L. Wong, Planar antennas for wireless communications, Wiley, New York, 2003.
21. SEMCAD, Schmid & Partner Engineering AG (SPEAG), Available at: http://www.semcad.com.
22. C.H. Chang and K.L. Wong, Printed λ/8-PIFA for penta-band WWAN operation in the mobile phone, IEEE Trans Antennas Propag 57 (2009), 1373–1381.
23. Y.W. Chi and K.L. Wong, Quarter-wavelength printed loop antenna with an internal printed matching circuit for GSM/DCS/PCS/UMTS operation in the mobile phone, IEEE Trans Antennas Propag 57 (2009), 2541–2547.
24. C.T. Lee and K.L. Wong, Internal WWAN clamshell mobile phone antenna using a current trap for reduced groundplane effects, IEEE Trans Antennas Propag 57 (2009), 3303–3308.

Ku-BAND MULTIWAY RECTANGULAR WAVEGUIDE POWER DIVIDER

Kaijun Song, Yong Fan, and Bo Zhang
EHF Key Laboratory of Fundamental Science, School of Electronic Engineering, University of Electronic Science and Technology of China, Chengdu, 610054, China; Corresponding author: kjsong@ee.uestc.edu.cn

Received 1 February 2010

ABSTRACT: *A novel multiway rectangular waveguide power divider using coaxial probe array has been presented. The model of the entire power divider has been introduced, and the effect of the higher order modes generated in the power divider has been discussed. A Ku-band eight-way rectangular waveguide power divider has been designed and fabricated. Good agreement between the simulated response and measurements was demonstrated. The measured 15-dB return loss and 1-dB insertion loss bandwidth of the power divider are all found to be about 7 GHz. The power divider developed is suitable for various applications of wide bandwidth.* © 2010 Wiley Periodicals, Inc.
Microwave Opt Technol Lett 52:2560–2563, 2010; View this article online at wileyonlinelibrary.com. DOI 10.1002/mop.25542

Key words: *multiway; rectangular waveguide; power divider; broadband; Ku-band*

1. INTRODUCTION

The power amplifier is a key element in microwave communication systems. The amplifier's bandwidth, output power, and efficiency drive the communication system's link performance, power budget, and thermal design. The traveling-wave tube amplifier, because of its high power capability and high efficiency, is widely used in microwave systems for radar, satellite communication, and wireless communication. However, motivated by benefits such as low supply voltage, small size, low development cost, and a wide commercial technology base, there is considerable interest in developing broadband, efficient, solid-state power amplifiers as an alternative to vacuum tube technology.

However, the individual solid-state devices produce less power and operate at lower efficiency as compared with individual vacuum tube devices. The power combining technique can integrate a large amount of amplifiers to obtain high output power and has been investigated actively [1–10].

In the previous studies, we developed a broadband multiway radial waveguide power divider/combiner. The design was elaborated upon [11, 12]. Based on equivalent-circuit approach, the electromagnetic modeling and design method of the power divider have been presented. The reported multiway radial power divider/combiner exhibits characteristics of small size, wide bandwidth, low loss, and good efficiency. However, higher order modes may be generated in the radial power dividing/combining cavity due to discontinuities, and cannot be suppressed effectively.

In this article, we presented a broadband mutliway power divider that employed a coaxial probe array and several rectangular waveguides. When the width and height of the rectangular waveguides satisfy the propagating conditions of the lowest order waveguide-type mode, the higher order modes are usually